

MORPHOGENESIS AND AGGRESSIVENESS OF CERVIX CARCINOMA

ELENA IZQUIERDO-KULICH*, MARGARITA AMIGÓ DE QUESADA**,
CARLOS MANUEL PÉREZ-AMOR*** AND JOSÉ MANUEL NIETO-VILLAR*

*Department of Physical-Chemistry, Faculty of Chemistry, University of Havana, Havana, Cuba

**Institute of Oncology and Radiobiology, Havana, Cuba

***Faculty of Physics, University of Havana, Havana, Cuba

(Communicated by Stefano Boccaletti)

ABSTRACT. A mathematical model was obtained to describe the relation between the tissue morphology of cervix carcinoma and both dynamic processes of mitosis and apoptosis, and an expression to quantify the tumor aggressiveness, which in this context is associated with the tumor growth rate. The proposed model was applied to Stage III cervix carcinoma *in vivo* studies. In this study we found that the apoptosis rate was significantly smaller in the tumor tissues and both the mitosis rate and aggressiveness index decrease with Stage III patients' age. These quantitative results correspond to observed behavior in clinical and genetics studies.

1. Introduction. The dynamics of the biological tissues depend on complex biochemical processes which stimulate the mitosis and apoptosis that occur at the level of individual cells. When both the DNA is damaged and the control cell control cycle mechanisms fail, mutations propagate out of control causing the appearance of cancer cells [1]. The diagnosis of cancer is based on clinical factors and tissue histopathological image which has a complex morphology that can be characterized through its fractal dimension [2], [3], [4]. In this sense, experimental results, although yet insufficient, seem to indicate that the tumor cell pattern's fractal dimension is greater than that of healthy tissue in the same location [5], [6], [7].

The virus responsible for cervix carcinoma is the papilloma virus HPV [8]. The morphology of this tumor tissue shows that both, nucleus/cytoplasm relation and cell density, are greater than in healthy cervix epithelium (Figure 1) [4]. Its prognosis depends on many factors such as the immune response and the clinical stage among others. In this sense, it has been observed that when this occurs in relatively young patients this type of cancer tends to be more aggressive [9].

A mathematical model was obtained to describe the relation between the tissue morphology of cervix carcinoma and both dynamic processes of mitosis and apoptosis at the level of individual cells. In this case, we take into account specifically

2000 *Mathematics Subject Classification.* 92C15, 82C31, 92C50.

Key words and phrases. Tumor growth, mesoscopic model, stochastic model, fractal, pattern cell morphology.

the cervix epithelium dynamics and the mathematical formalism applied in previous works, in which equations to predict the relation between the morphology and cancer dynamics were presented [10].

This paper is organized in the following way: in section 2, a mathematical model is presented; in section 3, the expressions to calculate both mitosis and apoptosis constant rate from the morphology were deduced from the model, and an equation to quantify the cervix cancer aggressiveness is proposed; in section 4, the obtained experimental results, when the proposed model was applied to cervix carcinoma *in vivo* studies, are shown and discussed; and finally the conclusions are presented.

2. Mesoscopic model. The cervix epithelium is a biological tissue which is kept under constant cell renewal [4]. The replication of the stem cells (Figure 1, A) produces well-differentiated cells (Fig. 1, B) which replace the apoptosis cells that are on the epithelium surface (Fig. 1, C). Due to the papilloma virus, the stem cells mutate and they produce not-differentiated cells (Fig. 1, D) which divide out of control.

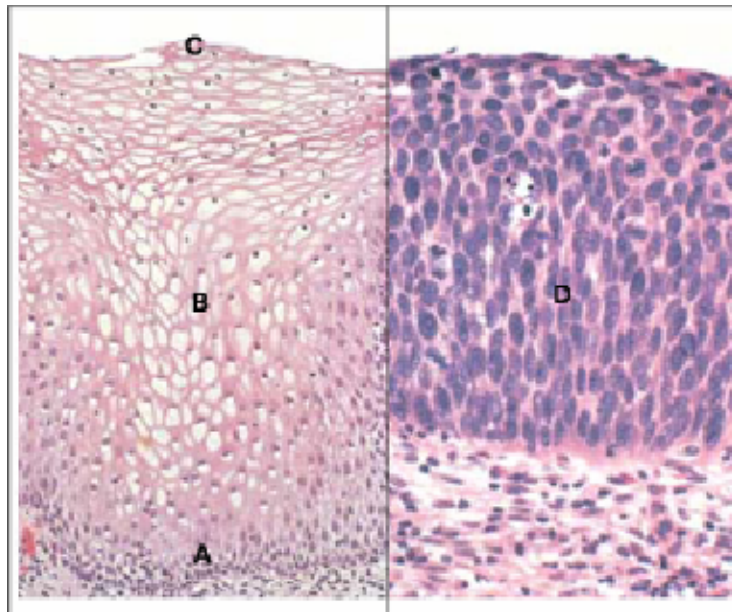


FIGURE 1. Histopathological image of a healthy cervix epithelium (left) and a cervix carcinoma (right). A: stem cells; B: well differentiated cells; C: apoptosis of cells on the surface of the cervix epithelium; D: not-differentiated cells of cervix carcinoma

The cervix carcinoma is visualized as a two-dimensional region (Figure 2) where tumor cells T proliferate and invade non-tumor tissue N , which usually is inflamed as a response to the invasion. The considered system to obtain the model is an area of arbitrary size Ω inside the tumor, which corresponds to the observed image used for diagnosis.

The microscopic variable is the total number of cells n inside Ω , and is suppose to change due to the following processes: i) the production of epithelium cells caused by

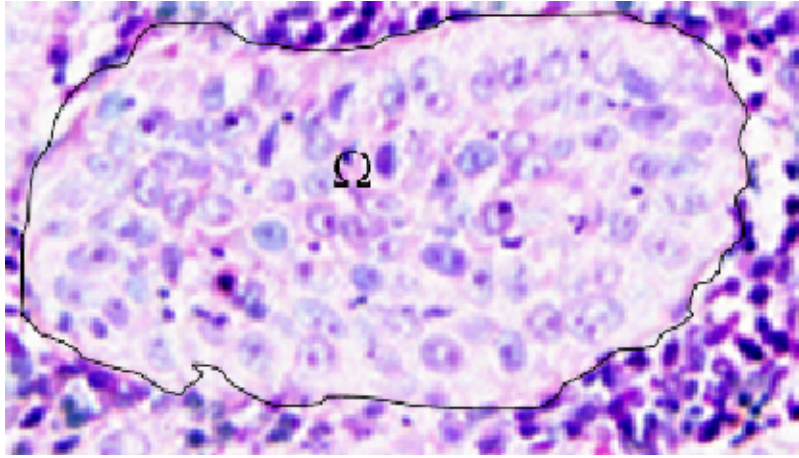


FIGURE 2. Considered system: two-dimensional region and area Ω occupied by tumor cells (T) which invade the inflamed non-tumor tissue N.

the division of stem cells, where the transition probability per unit of time $W_{1,n+1/n}$ is written as:

$$W_{1,n+1/n} = M; \quad (1)$$

ii) the mitosis process, whose transition probability per unit of time $W_{2,n+1/n}$ is given by:

$$W_{2,n+1/n} = k_1 n \quad (2)$$

and iii) the apoptosis due to the competition for space and nutrients, and the action of regulatory mechanisms, where the transition probability $W_{3,n-1/n}$ is assumed as:

$$W_{3,n-1/n} = \frac{k_2}{\Omega} n^2. \quad (3)$$

where M is a rate constant $[t^{-1}]$ associated with the division of stem cells, k_1 is the mitosis rate constant $[t^{-1}]$, and k_2 is the apoptosis rate constant $[t^{-1}]$.

The master equation [11] that describes the temporal behavior of the probability $P(n;t)$ of having cells n at time t is written from the transition probabilities per unit of time established *a priori*:

$$\begin{aligned} \frac{\partial P(n;t)}{\partial t} &= (E^{-1} - 1) M P(n;t) \\ &+ (E^{-1} - 1) k_1 n P(n;t) \\ &+ (E^{+1} - 1) \frac{k_2}{\Omega} n^2 P(n;t) \\ P(1;0) &= 1. \end{aligned} \quad (4)$$

If Ω is selected sufficiently large in such way that n can be considered as a continuous variable, then the step operator E^a can be expressed as [12]:

$$E^a = 1 + a \frac{\partial}{\partial n} + a^2 \frac{\partial^2}{\partial n^2} + \dots, \quad (5)$$

and substituting equation (5) in equation (4), the following Fokker-Planck equation is obtained:

$$\begin{aligned} \frac{\partial P(n;t)}{\partial t} = & -\frac{\partial}{\partial n} \left[\left(M + k_1 n - \frac{k_2}{\Omega} n^2 \right) P(n;t) \right] \\ & + \frac{1}{2} \frac{\partial^2}{\partial n^2} \left[\left(M + k_1 n + \frac{k_2}{\Omega} n^2 \right) P(n;t) \right]. \end{aligned} \quad (6)$$

The observed macroscopic variable is defined as the percentage x of Ω which is occupied by the cells:

$$x \equiv \epsilon \frac{n}{\Omega^*}, \quad (7)$$

where $\Omega = \frac{\Omega}{\epsilon}$ and ϵ is a constant which is related to the size of individual cell; taking into account the following relation between the probability $P(n;t)$ and the probability $\Pi(x;t)$ associated with the macroscopic variable [11]:

$$P(n;t) \partial n = \Pi(x;t) \partial x, \quad (8)$$

a change of variable was carried out on the Fokker-Planck equation (6), in such way that:

$$\begin{aligned} \frac{\partial \Pi(x;t)}{\partial t} = & -\frac{\partial}{\partial x} \left[(M + k_1 x - k_2 x^2) \Pi(x;t) \right] \\ & + \frac{1}{2} \frac{1}{\Omega^*} \frac{\partial^2}{\partial x^2} \left[(M + k_1 x + k_2 x^2) \Pi(x;t) \right]. \end{aligned} \quad (9)$$

is obtained.

Equation (9) is non-linear; therefore it is not possible to obtain an exact solution. Nevertheless, an approximate analytical solution can be obtained when we consider the dynamic behavior of the system in the vicinity of the stationary state, where $\Pi(x;t)$ is normal or Gaussian [11], [12]. In this case, the expected value is given by the differential equation:

$$\begin{aligned} \frac{d\langle x \rangle}{dt} &= M + k_1 \langle x \rangle - k_2 \langle x \rangle^2 \\ \langle x \rangle_{t=0} &= x_0, \end{aligned} \quad (10)$$

and the variance σ associated with the internal fluctuations is expressed as:

$$\begin{aligned} \frac{d\sigma}{dt} &= 2(k_1 - 2k_2 \langle x \rangle) \sigma + \frac{1}{\Omega^*} \left(M + k_1 \langle x \rangle + k_2 \langle x \rangle^2 \right) \\ \sigma(0) &= \sigma_0. \end{aligned} \quad (11)$$

Defining the non-dimensional time τ and non-dimensional parameters α and β :

$$\begin{aligned} \tau &= tM \\ \alpha &= \frac{k_1}{M}, \end{aligned} \quad (12)$$

$$\beta = \frac{k_2}{M}, \quad (13)$$

the differential equations (10) and (11) are written as:

$$\begin{aligned} \frac{d\langle x \rangle}{d\tau} &= 1 + \alpha \langle x \rangle - \beta \langle x \rangle^2 \\ \langle x \rangle_{\tau=0} &= x_0 \end{aligned} \quad (14)$$

$$\begin{aligned} \frac{d\sigma}{d\tau} &= 2(\alpha - 2\beta \langle x \rangle)\sigma + \frac{1}{\Omega^*} (1 + \alpha \langle x \rangle + \beta \langle x \rangle^2) \\ \sigma(0) &= \sigma_0, \end{aligned} \quad (15)$$

where:

$$\Pi(x; \tau) = \frac{1}{(2\pi\sigma)^{0.5}} \exp\left(-\frac{(x - \langle x \rangle)^2}{2\sigma}\right) \quad (16)$$

Equations (14), (15) and (16) describe the mesoscopic temporal behavior of the system in the vicinity of the stationary state [11].

3. Relationship among morphology, dynamics and aggressiveness. As the temporal averages are constant in the stationary state, we can assume that the stochastic process is ergodic [11], [12], in such way that temporal averages are equivalent to spatial averages. If the probability $\Pi^s(x) = \lim_{\tau \rightarrow \infty} \Pi(x; \tau)$ is visualized by an ensemble then the expected value $\langle \Pi^s(x) \rangle$ is proportional to the cell density inside Ω^* , so [10]:

$$\begin{aligned} \rho &= \langle \Pi^s(x) \rangle \\ &= \int (\Pi^s(x)) \Pi^s(x) dx \\ &= \frac{1}{(2\pi \exp(1) \sigma)^{0.5}}. \end{aligned} \quad (17)$$

If the mathematical definition of box counting fractal dimension D_f is taken into account [2], then we arrive to:

$$\begin{aligned} D_f &\equiv \lim_{x \rightarrow 1} \left(\lim_{\Omega \rightarrow x} \frac{d \ln \rho}{d \ln \frac{1}{x}} \right) \\ &\equiv \lim_{x \rightarrow 1} \left(\lim_{\Omega^* \rightarrow x} \frac{d \ln (2\pi \exp(1) \sigma)}{d \ln x} \right). \end{aligned} \quad (18)$$

where it was considered that the minimum box size is $x = 1$ corresponding to one individual cell and the system is visualized in a mesoscopic scale, where $\Omega^* \rightarrow x$ [10].

In order to express D_f as a function of the parameters α and β , it is necessary to write σ as a function of x . For this, the following differential equation is obtained from equations (14) and (15):

$$\begin{aligned} \frac{d\sigma}{dx} &= \frac{2(\alpha - 2.0\beta x)\sigma + \frac{1}{\Omega^*}(1 + \alpha x + \beta x^2)}{1 + \alpha x - \beta x^2} \\ \sigma(0) &= 0, \end{aligned} \quad (19)$$

where the series solution of the equation (19) is:

$$\begin{aligned} \sigma(x) &\approx \left(\frac{1}{\Omega^*}\right)x + \frac{\alpha}{\Omega^*}x^2 + \left(-\frac{0.00001}{\Omega^*}(\alpha^2 + 66666.\beta)\right)x^3 \\ &+ \left(-.33333\frac{\beta}{\Omega^*}\alpha\right)x^4 + O(x^5). \end{aligned} \quad (20)$$

Substituting equation (20) in equation (18) the following approximate relation among D_f , α , and β is obtained:

$$D_f \simeq \frac{1 + 2\alpha - 2\beta}{1 + \alpha - .66667\beta} \quad (21)$$

where the pattern cells fractal dimension D_f can be calculated with a suitable software for image processing. Besides D_f , another morphological parameter is necessary to be determined, because there are two unknown quantities, α and β . If we assume that $\langle x \rangle^s$ is associated with the percentage of black pixels λ of the binary histopathological images of the tumor tissue, where the nucleus cells are black, then:

$$\begin{aligned} \lambda &\equiv \langle x \rangle^s \\ &\equiv \frac{1}{2} \left(\frac{\alpha}{\beta} + \sqrt{\left(\frac{\alpha}{\beta}\right)^2 + \frac{4.0}{\beta}} \right), \end{aligned} \quad (22)$$

Therefore, the dynamic parameters α and β can be estimated from the morphological parameters λ and D_f , according to:

$$\alpha = \frac{.66667D - 2 + \lambda^2 - \lambda^2 D}{(\lambda D + 2 - 2\lambda - .66667D)\lambda} \quad (23)$$

$$\beta = \frac{\lambda D - \lambda + 2 - D}{(.66667D - \lambda D - 2 + 2\lambda)\lambda} \quad (24)$$

The histopathological image of a cervix carcinoma tissue and both, its corresponding black and white binary image and the cell pattern are shown in Figure 3.

In this context, the tumor aggressiveness is related to the tumor growth rate V , which depends on the values of α and β . In order to obtain an expression to quantify the aggressiveness, the temporal behavior of x is obtained from the analytical exact solution of the differential equation (14) for $x(0) = 1$:

$$x(\tau) = \frac{1}{2} \left(\frac{\alpha}{\beta} + \frac{\sqrt{(\alpha^2 + 4\beta)}}{\beta} \left(\tanh \left(\frac{1}{2}\tau\sqrt{(\alpha^2 + 4\beta)} + \gamma \right) \right) \right) \quad (25)$$

where $\gamma = \operatorname{arctanh} \frac{2\beta - \alpha}{\sqrt{(\alpha^2 + 4\beta)}}$.

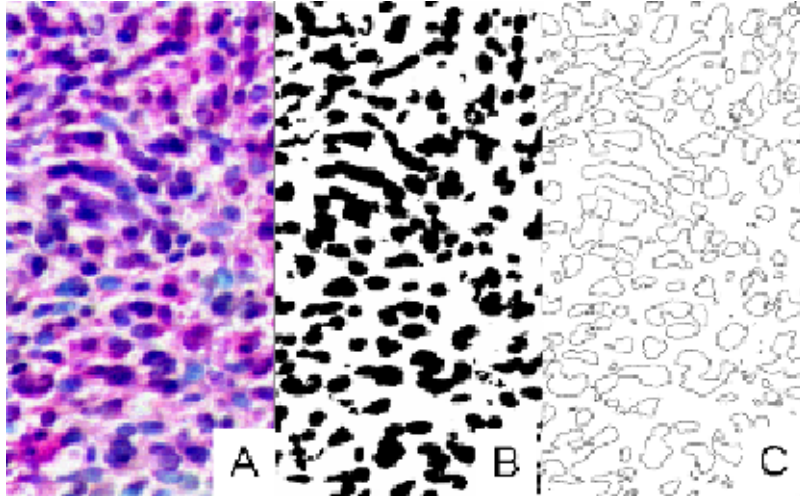


FIGURE 3. Image processing: A: histopathological image of tumor tissue; B binary image with $\lambda = 35\%$; C cell pattern with $D_f = 1.56$

If the tumor growth rate V is defined as $\frac{dx(\tau)}{d\tau}$, then V can be obtained from the temporal derivative of the equation (24):

$$V(\tau) = -\frac{0.25}{\beta} (\alpha^2 + 4.0\beta) \left(\tanh^2 \left(\gamma + 0.5\tau\sqrt{\alpha^2 + 4.0\beta} \right) - 1.0 \right) \quad (26)$$

As V changes with the time τ , the aggressiveness index is related to the value of V for an arbitrary time $\tau = \phi$. Taking into account that V reaches its maximum value when $x(\tau) \simeq \frac{\langle x \rangle^s}{2}$, ϕ is selected from the solution of the equation:

$$\frac{\langle x \rangle^s}{2} = \frac{1}{2} \left(\frac{\alpha}{\beta} + \frac{\sqrt{(\alpha^2 + 4\beta)}}{\beta} \left(\tanh \left(\frac{1}{2}\phi\sqrt{(\alpha^2 + 4\beta)} + \gamma \right) \right) \right), \quad (27)$$

in such way that:

$$\phi = \frac{2}{\sqrt{\alpha^2 + 4\beta}} \left(\operatorname{arctanh} \frac{(\alpha - 2\beta)}{\sqrt{\alpha^2 + 4\beta}} - \operatorname{arctanh} \frac{\alpha - 1.0\beta\sqrt{\frac{1}{\beta^2}(\alpha^2 + 4.0\beta)}}{4\sqrt{\alpha^2 + 4.0\beta}} \right) \quad (28)$$

Substituting $\tau = \phi$ in equation (26) we proposed an index Ψ to quantify the cervix carcinoma aggressiveness:

$$\Psi = .125 \frac{\alpha^2 + \alpha\sqrt{(\alpha^2 + 4.0\beta)} + 6.0\beta}{\beta} \quad (29)$$

where Ψ represents the maximum cell proliferation rate in a region Ω inside the tumor and, therefore, it must be related to the tissue growth rate.

4. Experimental obtained results and discussion. The proposed formalism was applied to quantify the cervix carcinoma aggressiveness *in vivo*. For this, 35 cases of stage III patients were selected, and considered the patients' age as the clinical parameter. The histopathological images of both the tumor tissues and

healthy cervix epithelium tissues, which were treated with hematoxylin-eosin tincion, were taken with a microscope Olympus CX21FS ($\times 40$) and an 8 mega pixels Canon digital camera. Each image was processed with the ImageJ 1.40g software by Wayne Rasband, National Institute of Health, USA (<http://rsb.info.nih.gov/ij>). For each case, 9 images were analyzed, where the maximum relative error associated to both λ and D_f was 2% and 4.5%, respectively.

The average values of λ and D_f corresponding to each case were used to estimate both the experimental value of α and β from equations (23) and (24). As the only considered clinical variable was the patient age g and many factor are known to influence the cancer aggressiveness [1], [13] cases were grouped according to their ages and g , α and β averages were calculated for each group. Then we applied statistical methods using the software STATGRAPHICS Plus 5.1 with the objective to study the correlation among g , α and β . The obtained results are shown on Figure 4 and 5.

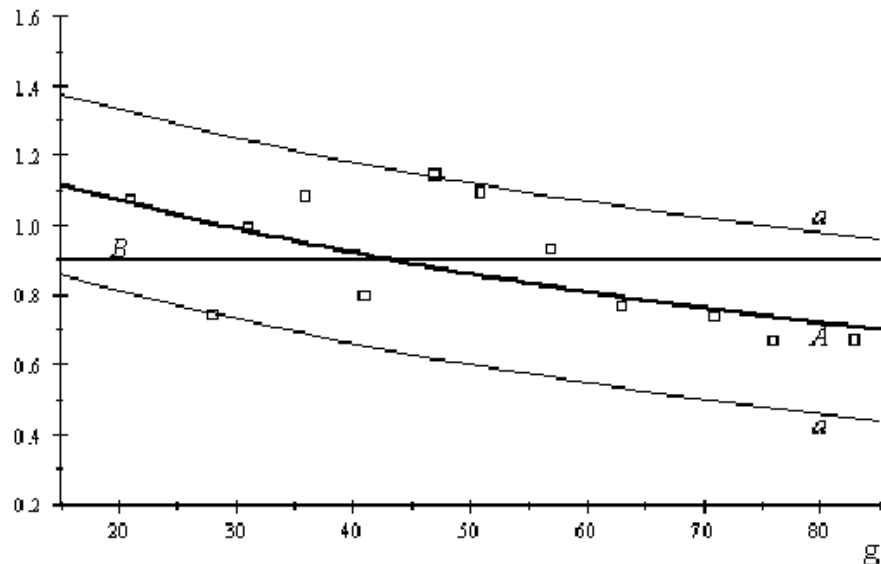


FIGURE 4. Experimental obtained results for the mitosis rate. (\square): Experimental mitosis rate with respect to patient age g ; A adjusted statistical model; a limits to prediction; B mitosis rate corresponding to a healthy cervix epithelium

The value of α average taking all cases is 0.9024, slightly greater than the one corresponding to a healthy epithelium cervix ($\alpha = 0.8885$). Nevertheless, the total average β is 0.035 for tumor tissues, whereas $\beta = 0.2163$ for the healthy tissues; the calculated apoptosis rate was significantly smaller in the tumor tissues. It is well-known that the expression of the protein p53 is inhibited by papilloma virus gene E6 and, as p53 plays an important role in the DNA reparation and the induction of the apoptosis process [8], [13] we must expect that the calculated apoptosis rate of the tumor cells must be smaller than the one corresponding to healthy cells, as it was found in this study.

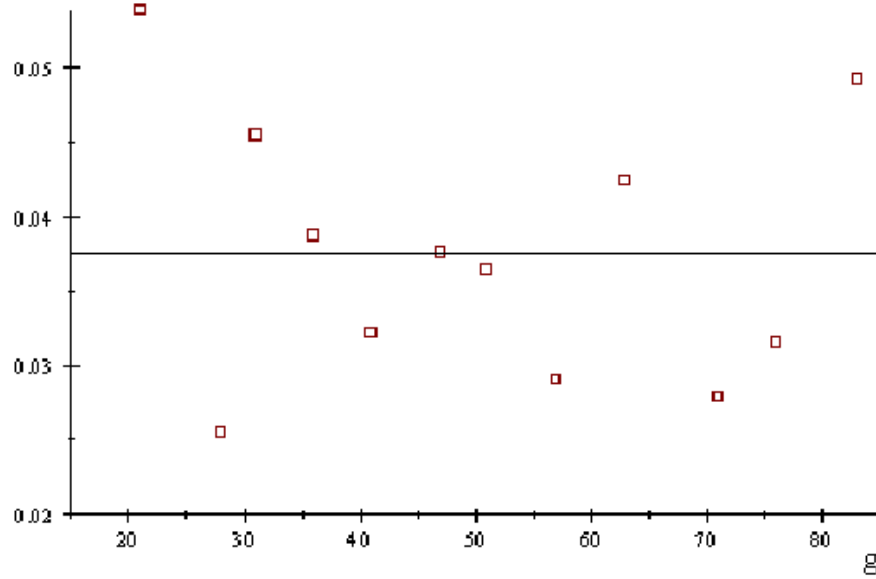


FIGURE 5. Experimental obtained result for the apoptosis rate β ; (\square) Experimental apoptosis rate with respect to patient age g ; (—) β average

The obtained statistical model for the relation between g and α is:

$$\alpha = \frac{1}{(0.781604 + 0.00760981g)} \quad (30)$$

The statistical analysis indicated that there is a significant statistical relation at the 95% confidence level, with a correlation coefficient of 0.812723, indicating a moderately strong relationship between α and g . The standard deviation of the residuals is 0.135176 and the statistical Durbin-Watson indicated that there is not serial correlation between residues. Therefore, the statistical model was accepted. According to this result, in this study we found that α decreases with the patient age, and it is interesting to observe that α corresponding to younger patient ($g \leq 45$) is greater than of a healthy cervix.

For the relation between β and g we found the statistical model:

$$\beta = 0.0309435 + \frac{0.280417}{g} \quad (31)$$

where the correlation coefficient is 0.20212, indicating a relatively weak relationship between β and g and there is not a significant statistical relations between and at the 90% or higher confidence level. Therefore, the statistical model (31) was rejected, and it is considered:

$$\begin{aligned} \beta &= \langle \beta \rangle \\ &= 0.035 \end{aligned} \quad (32)$$

Equations (30) and (32) were substituted in equation (29) to find the relation between both proposed aggressiveness index Ψ and the patient's age g . The obtained quantitative predictions are showed on Figure 6.

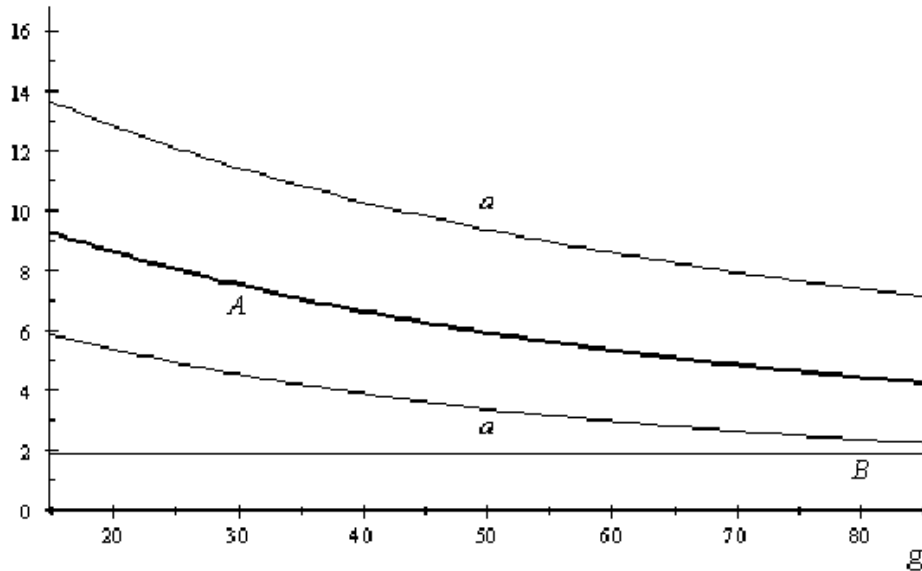


FIGURE 6. Aggressiveness index Ψ or tissue growth rate index with respect to the age g . A cervix carcinoma; a : limits to prediction; B healthy cervix epithelium

The obtained behavior predicts the following facts: i) the tumor tissue of cervix carcinoma has a growth rate at stage III ranging from 2.2 to 4.5 bigger than the corresponding to a healthy tissue. This result is logical if it is considered that the invasion of the normal tissue only is possible if the tumoral cells growth faster than the normal cells and ii) cervix carcinoma in older women is less aggressive, which corresponds with the clinical observation [9]. This fact can be explained as a result that the tumor mitosis rate decreased with age, according to the quantitative results obtained from the proposed equations. Therefore, we do not find enough evidence to reject the proposed model, at least for the cases *in vivo* considered in this study. Nevertheless, it is important to point out that this model has limitations, because only the patient's age was considered as a clinical factor, and there are many others such as the immune response, virus type, sociological aspects, clinical stage, etc, which can influence the aggressiveness and prognosis.

5. Conclusions and remarks. From a mesoscopic model obtained taking into account the specific dynamic processes that occur on cervix tissues, we obtained the equations to predict the mitosis and apoptosis rate in cervix carcinoma from the morphological characteristics of histopathological images; and an expression to quantify the tumor aggressiveness, which in this context is associated with the tumor growth rate. The obtained equations were used to study *in vivo* the behavior of aggressiveness with respect to clinical stage III patient's age. The experimental calculated results predicted that the apoptosis is the mechanism damaged as the

result of the infection with the papilloma virus corresponding with genetic studies [8], [9]. On the other hand, it is predicted that the cervix carcinoma aggressiveness decreases with age, which is corresponding with the observed results in clinical studies.

Acknowledgments We would like to thank Roger Rodriguez Cruz for their reading of the final manuscript. This work was supported by Spanish Agency of International Co-operation for Development (AECID, projects: D/023653/09 and D/030752/10)

REFERENCES

- [1] S. A. Frank, "Dynamics of Cancer," H. Allen Orr, Princenton, Series in evolutionary Biology, 2007.
- [2] J. W. Baish and R. K. Jain, *Fractals and cancer*, Cancer Res., **60** (2000), 3683–3688.
- [3] G. Landini, "Complexity in Tumour Growth Patterns," *Fractals in Biology and Medicine*, Vol. II, Birkhauser Verlag, Basel, 1998.
- [4] Robbins and Cotran, eds., "Pathologic Basis of Disease," Elsevier, 2005.
- [5] L. Norton, *Conceptual and practical implications of breast tissue geometry: Toward a more effective, less toxic therapy*, Oncologist, **10** (2005), 370–381.
- [6] E. Sabo, A. Boltenko, Y. Sova, A. Stein, S. Kleinhaus and M. B. Resnick, *Microscopic analysis and significance of vascular architectural complexity in renal cell carcinoma*, Clinical Cancer Research, **7** (2001), 533–537.
- [7] R. Sedivy, Ch. Windischberger, K. Svozil, E. Moser and G. Breitenecker, *Fractal analysis: An objective method for identifying atypical nuclei in dysplastic lesions of the cervix uteri*, Gynecologic Oncology, **75** (1999), 78–83.
- [8] E. M. Toledo Cuevas and A. García Carrancá, *P53 and human papillomavirus in the carcinogenesis of the uterine cervix*, Rev. Invest. Clín, **48**, (1996), 59–68.
- [9] T. Prempre, V. Patanaphan, W. Sewchand and R. M. Scott, *The influence of patients' age and tumor grade on the prognosis of carcinoma of the cervix*, Cancer, **51**, (1983), 764–177.
- [10] E. Izquierdo-Kulich, M. Amigó de Quesada, C. M. Pérez-Amor, M. Lopes Texeira and J. M. Nieto-Villar, *The dynamics of tumor growth and cells pattern morphology*, Mathematical Biosciences and Engineering, **6** (2009), 547–559.
- [11] N. G. van Kampen, "Stochastic Processes in Physics and Chemistry," N. H. Publications, Elsevier, 1992.
- [12] C. W. Gardiner, "Handbook of Stochastic Methods for Physics, Chemistry and the Natural Sciences," Third edition, Springer Series in Synergetics, **13**, Springer-Verlag, Berlin, 2004.
- [13] R. W. Tsang, A. W. Fyles, Y. Li, M. M. Rajaraman, W. Chapman, M. Pintilie and C. S. Wong, *Tumor proliferation and apoptosis in human uterine cervix carcinoma I: Correlations between tumor proliferation and apoptosis*, Radiother Oncol, **50** (1999), 85–92.

Received March 3, 2010; Accepted February 1, 2011.

E-mail address: elenaik@fq.uh.cu

E-mail address: mamigo@infomed.sld.cu

E-mail address: cp@fq.uh.cu

E-mail address: nieto@fq.uh.cu